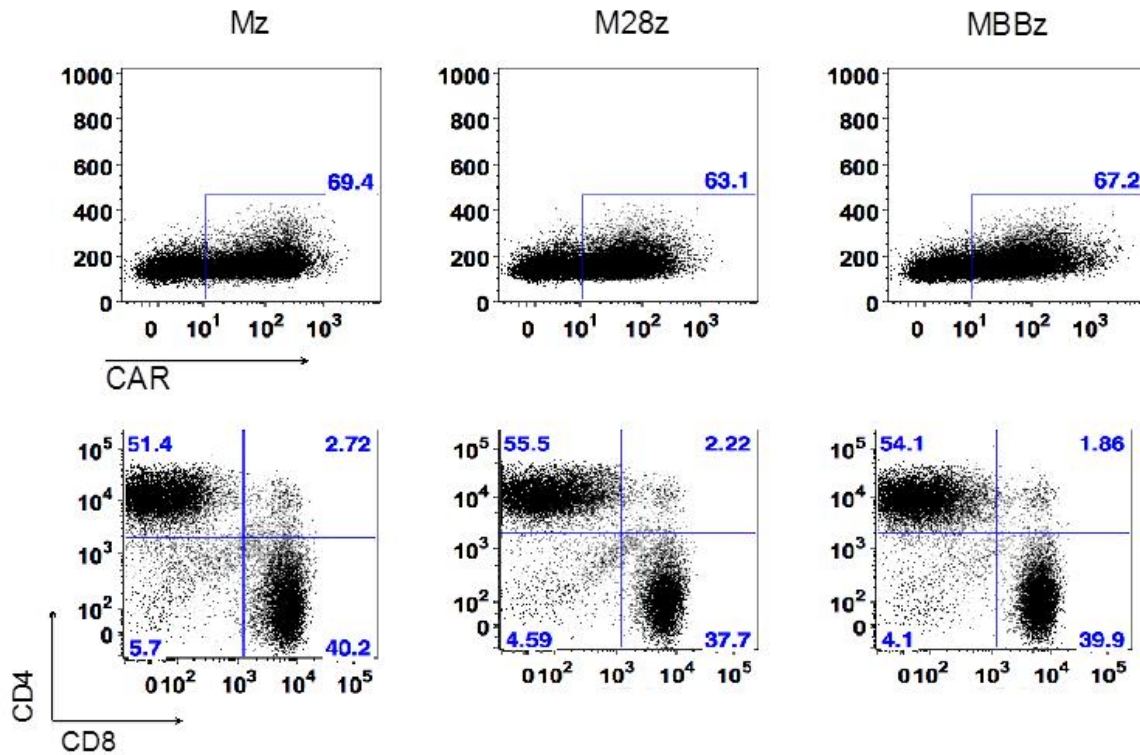


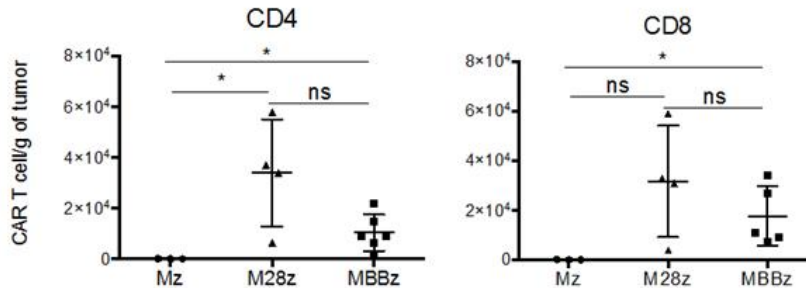
### Supplementary Figure 1.



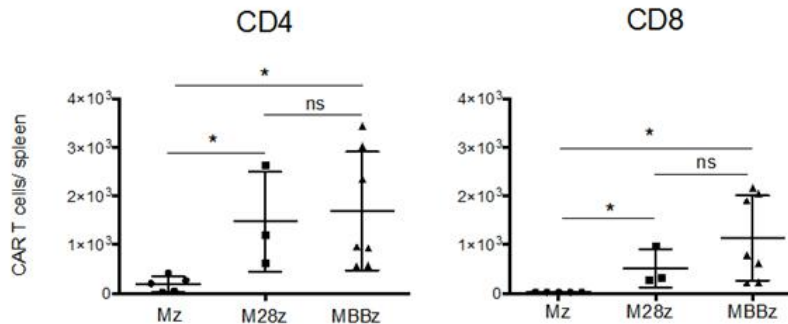
**Efficient retroviral transduction of human T cells to express Mz, M28z, and MBBz CARs.** (*Top*) Shown is representative FACS analysis 4 days after gene transfer. Fluorescence minus one staining was used to set positive gates after a live/dead stain excluded nonviable cells. All experiments used T cells with 50% to 70% CAR transduction efficiency; transduction percentages between T-cell groups were within 5% of each other. (*Bottom*) Both CD4+ and CD8+ T-cell subsets were efficiently transduced. CD4+ and CD8+ percentages after gating for CAR T cells are shown.

## Supplementary Figure 2.

### A CAR T-cell count in the Tumor, Day 6

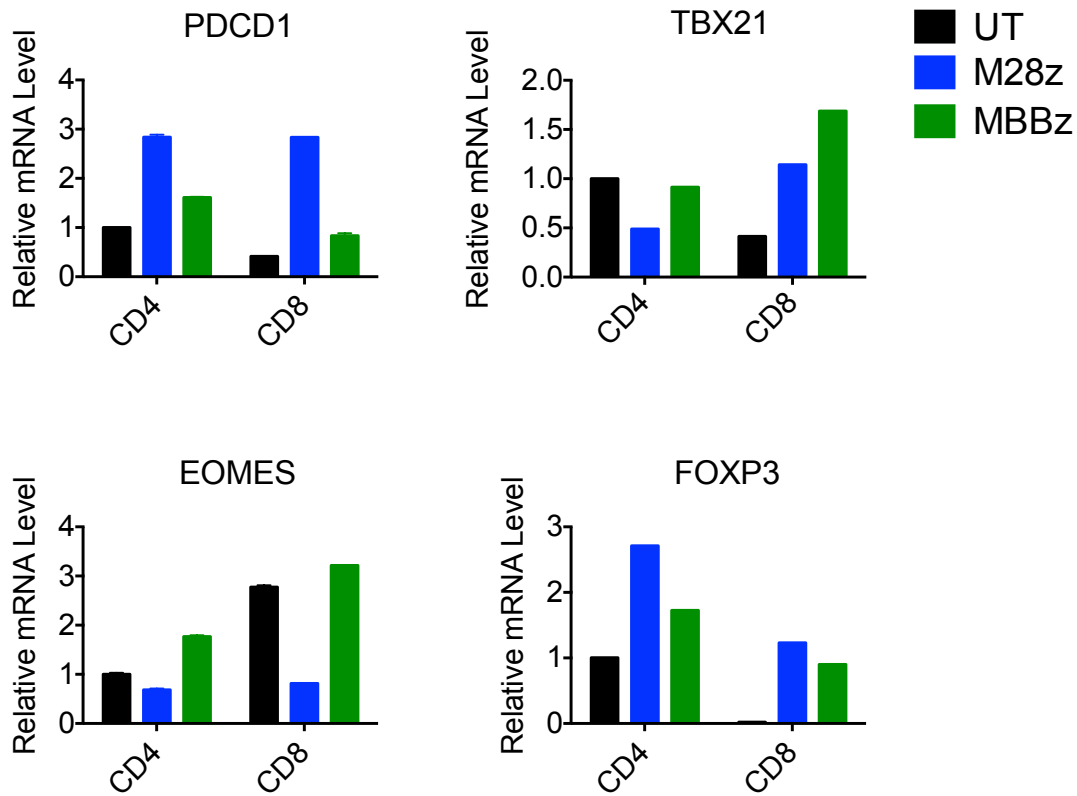


### B CAR T-cell count in the spleen, Day 74



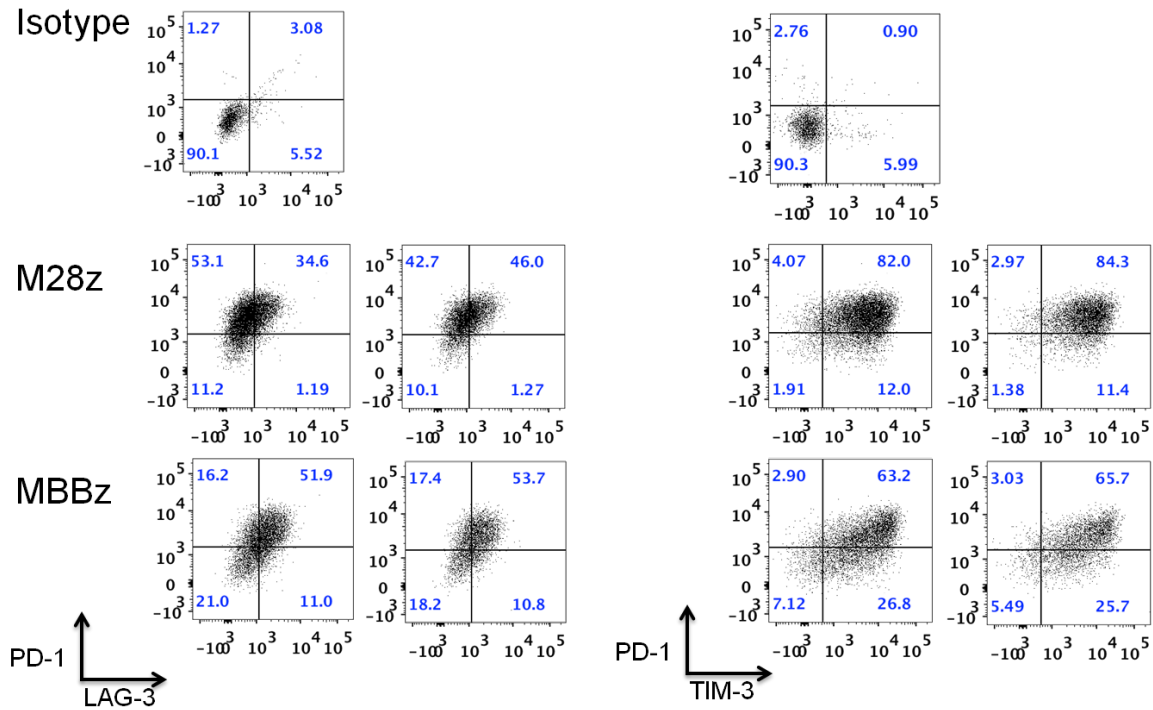
**M28z and MBBz CAR+ T cells demonstrated a similar early intratumoral accumulation and long-term persistence of both CD4+ and CD8+ T cells.** Mz, M28z, and MBBz CAR T cells were harvested from the tumor at Day 6 and spleen at Day 74 following T-cell administration into mice with pleural tumor. The absolute number (right panels) of CD4+ or CD8+ CAR T cells per gram of tumor (Panel A) or per spleen (Panel B) was quantified by flow cytometry using countbright absolute counting beads. Student's *t* tests were performed for statistical significance (\* $P < 0.05$ ).

**Supplementary Figure 3.**



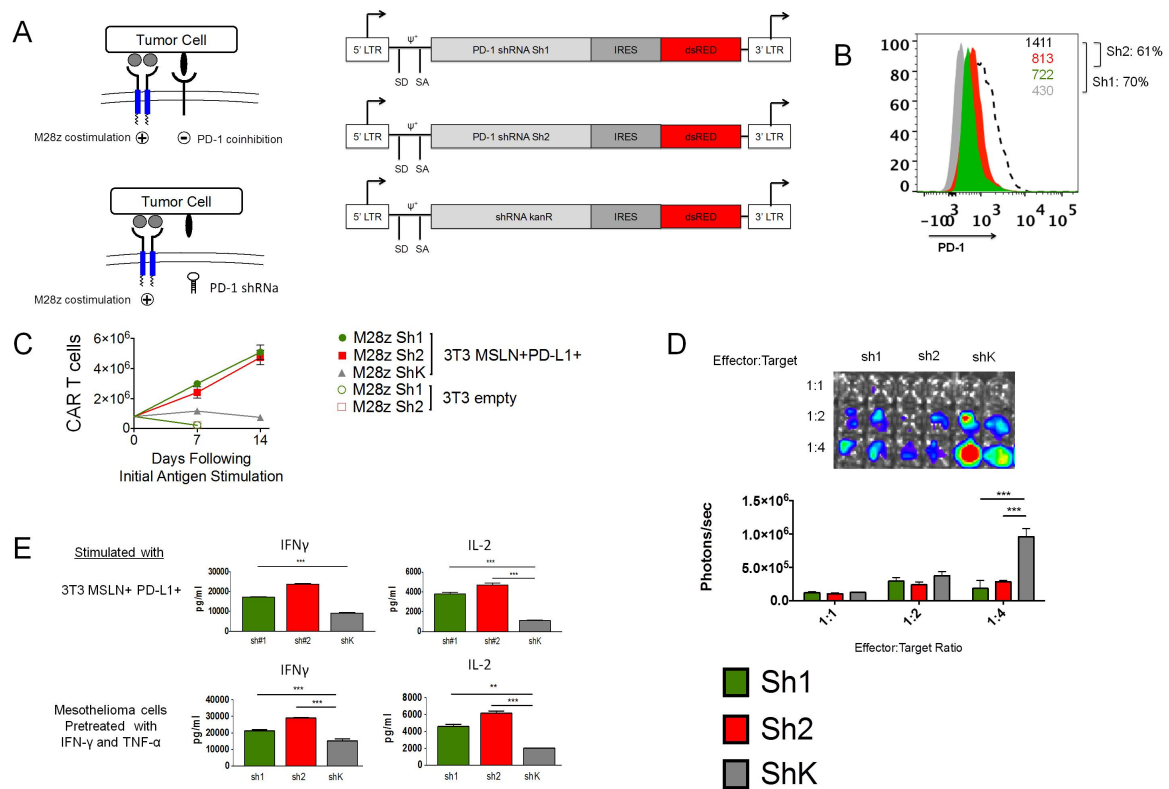
**MBBz CAR T cells express a less exhausted, more potent phenotype compared to M28z CAR T cells.** 4-1BB- and CD28-costimulated T cells were expanded with repeated antigen stimulation, and mRNA was extracted and subjected to RT-PCR analysis 20 h after the third stimulation. Data are represented in fold change relative to the mRNA expression of CD4+ untransduced T cells. MBBz CAR T cells express higher levels of *EOMES* (Eomesodermin) and *TBX21* (T-bet), and lower levels of *PDCD1* (PD-1) and *FOXP3* (Foxp3). All comparisons were significant at  $P < 0.001$ . Data are representative of at least 2 independent experiments.

### Supplementary Figure 4.



**Tumor-infiltrating M28z and MBBz CAR T cells coexpress PD-1 along with other inhibitory receptors.** At Day 6 after the administration of CAR T cells, the pleural tumor were harvested and CAR T cells were stained with CD3, CD45, LNGFR, PD-1 and Lag-3 (left panel) or Tim-3 (right panel). Isotype staining (top) was used as control to established positive gates

## Supplementary Figure 5.



**Cotransduction of PD-1 receptor–targeting shRNAs rescues M28z CAR T cells from PD-L1/PD-1–mediated inhibition *in vitro*.** (A) (Left) Schematic representation of CD28-costimulated T cells binding tumor-expressed PD-L1 via endogenous PD-1 receptor, with or without coexpression of PD-1–targeting shRNA. (Right) All experiments included M28z CAR T cells cotransduced with one of two PD-1–targeting shRNAs (sh1 or sh2 coexpressing a dsRED reporter) or with an shRNA targeting a bacterial sequence (KanR). (B) Compared with KanR-transduced cells, M28z CAR T cells cotransduced with PD-1–targeting shRNAs demonstrated a 60% to 70% knockdown in PD-1 receptor protein expression upon stimulation with phytohemagglutinin. Cells were incubated with either 3T3 fibroblasts overexpressing PD-L1 (3T3 MSLN+ PD-L1+)

or mesothelioma tumor cells that had been treated with IFN-g and TNF-a in order to upregulate PD-L1 and PD-L2. M28z PD1 shRNA CAR T cells demonstrate enhanced accumulation upon repeated antigen stimulation **(C)**, enhanced cytolytic function at low effector to target ratios, as measured by luciferase activity of remaining live tumor cells **(D)**, and increased Th1 cytokine secretion **(E)** (\*\* $P < 0.01$ ; \*\*\* $P < 0.001$ ). Student's *t* tests were performed and statistical significance was determined using the Sidak-Bonferonni correction for multiple comparisons. Data represent the mean  $\pm$  SEM of three replicates and are representative of at least 3 independent experiments.